

Momentum-space coupled-channels optical method for electron-atom scattering

I. E. McCarthy and A. T. Stelbovics

Institute for Atomic Studies, The Flinders University of South Australia, Bedford Park, South Australia 5042, Australia

(Received 28 January 1983)

A complete account is given of a new method for the solution of the problem of electron scattering by a one-electron atom or ion. The method treats all relevant effects explicitly. Reaction channels under consideration are treated by the coupled-channels method in momentum space. Other channels, including the continuum, are treated by adding complex-polarization potentials computed from experimentally tested approximate amplitudes for the relevant reactions. Computational methods are discussed in detail since this is the first successful application of the momentum-space solution to the atomic multichannel problem. The effect of the inclusion of channels outside the coupled space is demonstrated by comparison with three-state close coupling for hydrogen at 54.42 eV.

I. INTRODUCTION

Momentum-space methods in scattering theory are intrinsically appealing, since the basic quantities involved are scattering amplitudes. Experiments involve momentum measurements and, therefore, these quantities are quite directly related to experimental data. The simplest momentum-space calculation is the Born approximation.

The present paper gives the formalism, computational detail, and evaluation of approximations for an electron-atom scattering theory that is complete in the sense that all relevant effects are treated explicitly. The basic method is the coupled-channels method in momentum space, which involves the solution of a set of coupled Lippmann-Schwinger integral equations, one for each of a finite set of reaction channels. The driving term for each channel is the corresponding Born amplitude. The complete problem includes target-continuum channels and the remainder of the discrete channels. The continuum is taken into account by adding the corresponding complex-polarization potential,¹ calculated explicitly as an integral over continuum states, to the diagonal interchannel coupling potentials. The remaining discrete channels that contribute significantly are taken into account by explicit second-order polarization potentials. The present discussion is restricted to one-electron atoms, in which all but one electron constitute a closed-shell core, assumed to be inert for the purposes of the calculation. We have essentially a three-body problem. The extension to many-electron atoms will be given separately.

Momentum-space formulations of electron-atom scattering theory have been given, for example, by Mittleman and Watson,² Bonham,³ and Byron and Joachain.⁴ Calculations have usually been based on second-order solutions of the integral equations. The integral equation formalism has been discussed in detail by Sloan and Moore.⁵ Direct solutions of the integral equations for a small set of channels using the unitarized Born approximation (UBA) in atomic hydrogen have been performed by Burke and Seaton,⁶ who omitted exchange amplitudes. This type of calculation can be extended by including more channels⁷ and putting in exchange potentials.⁸ The earliest reported solutions of the full equations for two- and three-state close coupling followed much later in 1976

(Refs. 9 and 10) and are of limited scope.

Coupled-channels calculations for atomic scattering have usually been done in coordinate space, where they amount to the solution of a set of coupled integro-differential equations in a strongly coupled internal region, with boundary conditions given by solving a set of equations in the external region which are still coupled because of the long range of the dipole coupling potentials. Such calculations have been done, for example, by Kingston, Fon, and Burke,¹¹ who coupled the $1s$, $2s$, and $2p$ channels for atomic hydrogen.

Channels not included in the discrete physical set have been taken into account by expansions in square-integrable pseudostates. Pseudostates, whose purpose is to mimic the effects of higher-energy channels, are either included in the coupled-channels calculation, as has been done by Callaway, McDowell, and Morgan,¹² or in a calculation of the corresponding polarization potential as has been done by Scott and Bransden¹³ and Bransden, Scott, Shingal, and Roychoudhury.¹⁴ These examples again consider the $1s$, $2s$, and $2p$ channels for atomic hydrogen.

The present method may be summarized as follows. The coupled integral equations are solved by matrix methods using Gaussian quadratures to make them discrete. The driving terms and potential factors in the kernels consist of matrix elements of the coupling potentials. These are essentially Born matrix elements (both on- and off-shell). Target wave functions are approximated by single-electron excitations (orbital approximation). Each orbital is represented by a linear combination of Slater-type orbitals. Direct matrix elements are computed from analytic integrals for pairs of Slater-type orbitals. Exchange matrix elements are computed by numerical integration using the coordinate-space representation. Polarization-potential matrix elements are computed in momentum space with the use of the equivalent local approximation. They contribute only for cases which are diagonal in the channels. Amplitudes in the polarization-potential calculation for the continuum are computed in the extreme-screening (Born-Oppenheimer) approximation with the use of the Bonham-Ochkur¹⁵ approximation for exchange amplitudes. For discrete channels they are computed in the Born approximation with Bonham-Ochkur exchange.

The approximations involved in calculating the continuum polarization potentials have been discussed in Ref. 1. Details of the calculation of discrete polarization potentials have been given by McCarthy, Saha, and Stelbovics.^{16,17}

The single-channel version of the present theory for hydrogen has been extremely successful,¹⁸ reproducing entrance-channel data (elastic differential cross sections and total reaction cross sections) essentially within experimental error at 50, 100, and 200 eV. The coupled-channels optical calculation for the 1s, 2s, and 2p channels of hydrogen at the same energies has been equally successful for differential and total cross sections for each channel.¹⁹ The angular correlation parameters λ and R are not reproduced as well at backward angles for 54.4 eV, but this theory works better than any other.

The scope of the present paper is to give a detailed account of the coupled-channels optical (CCO) method which would enable it to be repeated by other workers. The formal theory is summarized in Sec. II. Sections III–VII give computational details for the various components of the calculations. Section VIII discusses the special problems in numerical analysis which occur in the atomic problem as distinct from the momentum-space problem with short-range two-body forces. It gives estimates of the numerical accuracy obtainable with different quadrature meshes in the three-state close-coupling problem for hydrogen at 54.42 eV. Section IX discusses the effect of the inclusion of the polarization potentials in comparison with three-state close coupling.

II. SUMMARY OF FORMAL THEORY AND NOTATION

The Hamiltonian for electron scattering on a one-electron target is

$$H = K_1 + K_2 + v_1 + v_2 + v_3, \quad (1)$$

where K and v stand for kinetic-energy and potential operators, respectively. We neglect the kinetic energy of the massive core. Subscripts 1 and 2 label the electron-core subsystems for electrons 1 and 2, respectively. v_3 is the electron-electron potential. We ignore spin-orbit coupling so that electron spin plays a part only in applying the Pauli exclusion principle. For the two-electron problem the total wave function is labeled by the total electron spin S and a number n that denotes the three-body quantum state with respect to the quantum numbers of bound states and momenta of positive-energy electrons. This is a discrete notation for the continuum in the cases where one or two electrons have positive energy with momenta \vec{q}_1, \vec{q}_2 . The discrete notation involves the usual box normalization and limits as the box is expanded. The Schrödinger equation for total energy E is

$$\{E^{(\pm)} - [K_1 + K_2 + v_1 + v_2 + v_3 + (-1)^S(H - E)P_r]\} \Psi_{nS}^{(\pm)} = 0, \quad (2)$$

where P_r is the space-exchange operator and the superscripts (\pm) denote outgoing and ingoing spherical-wave boundary conditions, respectively. Since singlet and triplet scattering are independent we suppress the index S to simplify the notation and use the abbreviation

$$v'_3 = v_3 + (-1)^S(H - E)P_r. \quad (3)$$

The reaction channels j are labeled by the one-electron target bound-state functions ϕ_j , which are Hartree-Fock functions in the case of alkali metals. We choose the label 2 for the bound electron. The space-exchange operator takes care of antisymmetry:

$$(\epsilon_j - K_2 - v_2)\phi_j = 0. \quad (4)$$

We use an operator notation where all operators are understood to act on the wave function $\Psi_n^{(+)}$. The Schrödinger equation (2) is written as

$$E^{(+)} - K = v, \quad (5)$$

where

$$K = K_1 + K_2, \\ v = v_1 + v_2 + v'_3. \quad (6)$$

We use projection operators P, Q for the sets P, Q of states

$$P = \sum_{i \in P} |\phi_i\rangle \langle \phi_i|, \quad Q = 1 - P \quad (7)$$

to separate the Schrödinger equation (5) into two projected equations

$$P(E^{(+)} - K - v)P = PvQ, \\ Q(E^{(+)} - K - v)Q = QvP. \quad (8)$$

The states in P space are a finite set including the ground state ϕ_0 . Q space includes the continuum and the remaining discrete states.

We formulate the coupled-channels problem for P space, with Q space eliminated by defining an optical potential $V^{(Q)}$ given by

$$V^{(Q)} = v_1 + v'_3 + (v_1 + v'_3)Q \frac{1}{Q(E^{(+)} - K - v)Q} Q(v_1 + v'_3). \quad (9)$$

The last term in (9) is the complex-polarization potential.

The coupled equations in P space are

$$P(E^{(+)} - K - v_2 - V^{(Q)})P = 0. \quad (10)$$

They are written in momentum space, with the use of an expanded notation, as

$$\sum_{j \in P} \langle \vec{k}_r \phi_i | E_i^{(+)} - K_1 - V^{(Q)} | \phi_j u_j^{(+)}(\vec{k}_j) \rangle = 0, \quad i \in P \quad (11)$$

where

$$|\phi_j u_j^{(+)}\rangle \equiv |\phi_j\rangle \langle \phi_j | \Psi_n^{(+)}\rangle, \\ E_i^{(+)} \equiv E^{(+)} + \epsilon_i, \quad (12)$$

and n stands for the set of states j, \vec{k}_j . Note the distinction between the momenta \vec{k}_i which correspond to the channel kinetic energy E_i of (12), and are thus "on-shell" and the \vec{k}_r which are not constrained. The corresponding set of coupled integral equations is written in operator notation as

$$T_{ij} = V_{ij} + \sum_{l \in P} V_{il} G_l T_{lj}, \quad (13)$$

or, in terms of explicit matrix elements, as

$$\langle \vec{k}_r, \phi_i | T | \phi_j, \vec{k}_j \rangle = \langle \vec{k}_r, \phi_i | V^{(Q)} | \phi_j, \vec{k}_j \rangle + \sum_{l \in P} \int d^3 k_r \langle \vec{k}_r, \phi_i | V^{(Q)} | \phi_l, \vec{k}_r \rangle \frac{1}{E^{(+)} - \epsilon_l - \frac{1}{2} k_r^2} \langle \vec{k}_r, \phi_l | T | \phi_j, \vec{k}_j \rangle, \quad (14)$$

where

$$T_{ij} \equiv \langle \vec{k}_r, \phi_i | T | \phi_j, \vec{k}_j \rangle = \langle \vec{k}_r, \phi_i | V^{(Q)} | \phi_j, u_j^{(+)}(\vec{k}_j) \rangle \quad (15)$$

is the T -matrix element for the transition from the channel state $|\phi_j, \vec{k}_j\rangle$ to $|\phi_i, \vec{k}_r\rangle$. Note that \vec{k}_r is an arbitrary momentum. The half-off-shell T -matrix element that is the solution of (14) contains the same physical information as the wave function $\langle \vec{k}_r | u_j^{(+)}(\vec{k}_j) \rangle$.

The optical potential matrix element is fully expanded as

$$\langle \vec{k}_r, \phi_i | V^{(Q)} | \phi_j, \vec{k}_r \rangle = \langle \vec{k}_r, \phi_i | v_1 + v_3' | \phi_j, \vec{k}_r \rangle + \sum_m \sum_{l' \in Q} \langle \vec{k}_r, \phi_i | v_3' | \phi_l \rangle \langle \phi_l | \Psi_m^{(-)} \rangle \frac{1}{E^{(+)} - E_m} \langle \Psi_m^{(-)} | \phi_l \rangle \langle \phi_l | v_3' | \phi_j, \vec{k}_r \rangle. \quad (16)$$

The one-electron bound state is written in terms of a Slater expansion which in coordinate- and momentum-space, respectively, takes the form

$$\langle \vec{r} | n, l, m \rangle = \sum_{\mu} c_{\mu} A_{\mu} r^{n_{\mu}-1} \exp(-\xi_{\mu} r) Y_{lm}(\hat{r}), \quad (17a)$$

$$\langle \vec{p} | n, l, m \rangle = i^l \left(\frac{2}{\pi} \right)^{1/2} \frac{1}{p} \sum_{\mu} c_{\mu} A_{\mu} n_{\mu}! \left[\text{Im} \frac{1}{(\xi_{\mu} - ip)^{n_{\mu}+1}} \right] Y_{lm}(\hat{p}), \quad (17b)$$

where

$$A_{\mu} = \left[\frac{(2\xi_{\mu})^{2n_{\mu}+1}}{(2n_{\mu})!} \right]^{1/2}, \quad (18)$$

$$|\phi_j\rangle \equiv |n, l, m\rangle, \quad |\phi_i\rangle \equiv |n', l', m'\rangle. \quad (19)$$

Here the symbols n, l, m have their usual meanings as one-electron quantum numbers. No confusion should arise with their use as formal channel indices in, for example, Eq. (16).

For computation we make a partial-wave expansion of the T - and V - matrix elements, defining the partial matrix elements $T_{nLl}^{n'L'l'(J)}(k_r, k_r')$ for total angular momentum quantum number J by

$$\langle \vec{k}_r; n', l', m' | T | n, l, m; \vec{k}_r \rangle = \sum_{L, M, L', M', J, K} \langle \hat{k}_r | L', M' \rangle C_{L'LJ}^{M'm'K} \times T_{nLl}^{n'L'l'(J)}(k_r, k_r') C_{L'LJ}^{MmK} \langle L, M | \hat{k}_r \rangle, \quad (20)$$

where

$$\langle \hat{k} | L, M \rangle \equiv Y_{LM}(\hat{k}) \quad (21)$$

and $C_{L'LJ}^{MmK}$ is a Clebsch-Gordan coefficient. The definition of $V_{nLl}^{n'L'l'(J)}$ is analogous to (20) with $V^{(Q)}$ substituted for T . We suppress the superscript (Q) where this causes no confusion.

III. CROSS SECTIONS AND OTHER EXPERIMENTAL QUANTITIES

The differential cross section for scattering from channel j to channel i at an angle θ is

$$\frac{d\sigma_{ij}}{d\Omega} = (2\pi)^4 \frac{k_i}{k_j} \frac{\hat{S}^2}{\hat{l}^2} \sum_{m, m'} |\langle \vec{k}_i; n', l', m' | T | n, l, m; \vec{k}_j \rangle|^2, \quad (22)$$

$$\langle \vec{k}_i; n', l', m' | T | n, l, m; \vec{k}_j \rangle = \sum_{L, L', J} (4\pi)^{-1} \hat{L}' \hat{L} \left[\frac{(L' - |M'|)!}{(L' + |M'|)!} \right]^{1/2} \Theta(M') \times C_{L'LJ}^{M'm'm} C_{L'LJ}^{0mm} T_{nLl}^{n'L'l'(J)} P_L^{|M'|}(x), \quad (23)$$

where

$$\begin{aligned} \hat{l} &= (2l+1)^{1/2}, \\ \Theta(M') &= 1, \quad M' < 0 \\ \Theta(M') &= (-1)^{M'}, \quad M' \geq 0 \\ x &= \cos\theta. \end{aligned} \quad (24)$$

The corresponding total cross section is

$$\sigma_{ij} = (2\pi)^4 \frac{k_i}{k_j} \frac{\hat{S}^2}{\hat{l}^2} \frac{1}{4\pi} \sum_{L, L', J} (2J+1) |T_{nLl}^{n'L'l'(J)}|^2. \quad (25)$$

We have omitted the on-shell momentum arguments of the partial T -matrix elements for brevity of notation.

The differential cross section converges quite slowly with J at intermediate energies but there is a value J_0 beyond which the Born approximation

$$T_{nLl}^{n'L'l'(J)} = V_{nLl}^{n'L'l'(J)} \quad (26)$$

is sufficiently accurate. One can use this fact to calculate the differential cross section using the closed-form expression for the Born approximation by substituting in (22) to

write the T matrix in the form

$$\begin{aligned} \langle \vec{k}_i; n', l', m' | T | n, l, m; \vec{k}_j \rangle \\ = \langle \vec{k}_i; n', l', m' | (T - V) | n, l, m; \vec{k}_j \rangle \\ + \langle \vec{k}_i; n', l', m' | V | n, l, m; \vec{k}_j \rangle. \end{aligned} \quad (27)$$

The partial-wave expansion is used for the first term up to J_0 [in view of (26) its partial-wave expansion is essentially

$$\begin{aligned} \langle \vec{k}_i; n', l', m' | v_3 | n, l, m; \vec{k}_j \rangle = [2\pi^2 K^2]^{-1} \sum_{\lambda} i^{\lambda} \hat{\lambda}^2 \hat{l} \Theta(\mu) (-1)^l \left[\frac{(\lambda - |\mu|)!}{(\lambda + |\mu|)!} \right]^{1/2} \\ \times C_{\lambda l' l}^{\mu m' m} \begin{Bmatrix} \lambda & l' & l \\ 0 & 0 & 0 \end{Bmatrix} \left\{ \sum_N g_{\lambda}^N(\alpha_N, K) \right\} P_{\lambda}^{|\mu|}(x). \end{aligned} \quad (29)$$

The factor in braces is the radial integral for a pair of Slater functions, one in ϕ_i and one in ϕ_j [see Eqs. (17)] summed over pair indices N . The factor in parentheses is a Wigner 3- j symbol. Here

$$g_{\lambda}^N(\alpha_N, K) = C_N \int_0^{\infty} dr j_{\lambda}(Kr) r^N \exp(-\alpha_N r), \quad (30)$$

where

$$\begin{aligned} N &= n_{\mu} + n_{\mu'}, \\ C_N &= c_{\mu} c_{\mu'} A_{\mu} A_{\mu'}, \\ \alpha_N &= \xi_{\mu} + \xi_{\mu'}, \\ \vec{K} &= \vec{k} - \vec{k}'. \end{aligned} \quad (31)$$

Evaluating the integral (30) yields

$$\begin{aligned} g_{\lambda}^N(\alpha, K) = C_N \left[\frac{\pi}{2K} \right]^{1/2} \frac{(K/2)^{\nu} \alpha \Gamma(\mu + \nu)}{(\alpha^2 + K^2)^{(1+\mu+\nu)/2} \Gamma(1+\nu)} \\ \times {}_2F_1 \left[\frac{2+\nu-\mu}{2}, \frac{1+\nu+\mu}{2}, 1+\nu; \frac{K^2}{\alpha^2 + K^2} \right], \end{aligned} \quad (32)$$

where

$$\begin{aligned} \nu &= \lambda + \frac{1}{2}, \\ \mu &= N + \frac{1}{2}, \end{aligned} \quad (33)$$

and ${}_2F_1$ is the hypergeometric function.

The Coulomb part of the electron-core potential v_1 is a local, central potential:

$$\begin{aligned} \langle \vec{k}_i; n', l', m' | v_1 | n, l, m; \vec{k}_j \rangle \\ = [2\pi^2 K^2]^{-1} (-Z) \delta_{nn'} \delta_{ll'} \delta_{mm'}. \end{aligned} \quad (34)$$

Z is the core charge which is 1 in the case of a neutral target.

The momentum representations of v_1 and v_3 [Eqs. (29) and (34)] indicate a singularity at $K=0$ in the diagonal channels (i.e., when $i=j$). For neutral targets ($Z=1$) this singularity is canceled in the sum $v_1 + v_3$ so that the final potentials are nonsingular. To make this explicit we note that one can use the alternative representation of v_1 which is obtained by replacing $g_{\lambda}^N(\alpha_N, K)$ with $g_{\lambda}^N(\alpha_N, 0)$ in Eq.

zero for $J > J_0$. For the second term we use the closed-form expression for the Born approximation, writing the potential as

$$V = v_1 - (U + iW) + v_3, \quad (28)$$

where the term in parentheses is a local central potential found by approximating the complex-polarization part of the optical potential as described in Sec. VII. The amplitude for v_3 is given by

(29) and multiplying by -1 to take account of the attractive core-electron potential.

Since v_1, v_3, U , and W are all local central potentials, so is their sum V in Eq. (28). In a practical calculation U and W are found numerically as a function of K at a set of predetermined points. A momentum profile for all other points is determined by interpolation.

The angular correlation parameters λ and R for the excitation of different m components of a p state, when the ground state of the target is an s state, are given by

$$\lambda = |f_0|^2 / \sum_{m'} |f_{m'}|^2, \quad (35)$$

$$R = \text{Re}(f_0 f_1^*) / \sum_{m'} |f_{m'}|^2, \quad (36)$$

where

$$f_{m'} \equiv \langle \vec{k}_i; n', 1, m' | T | n, 0, 0; \vec{k}_0 \rangle. \quad (37)$$

For the entrance channel we must calculate the total reaction cross section σ_R in addition to the differential cross section. The S -matrix element is given in terms of the phase shift δ_j and the elastic T -matrix element:

$$S_j = \exp(2i\delta_j) = 1 - 2\pi i k_0 T_{nJ_0}^{nJ_0(J)}. \quad (38)$$

The total reaction cross section is

$$\sigma_R = (\pi/k_0^2) \sum_S (2S+1) \sum_J (2J+1) (1 - |S_J|^2). \quad (39)$$

Since the partial-wave expansion of σ_R may be slowly convergent with J , we make use of the fact that the Born approximation to σ_R is related to the imaginary part of the optical potential for $K=0$ by

$$\sigma_R^{\text{Born}} = (2/k_0)(2\pi)^3 W(0). \quad (40)$$

For $J > J_0$ the Born approximation (26) is valid. The total reaction cross section is, therefore, calculated by

$$\begin{aligned} \sigma_R = (\pi/k_0^2) \sum_S (2S+1) \sum_{J \leq J_0} (2J+1) (|S_J^{\text{Born}}|^2 - |S_J|^2) \\ + \sigma_R^{\text{Born}}. \end{aligned} \quad (41)$$

IV. SOLUTION OF THE COUPLED INTEGRAL EQUATIONS

The partial-wave expansion of the set (14) of coupled Lippmann-Schwinger equations results in closed sets of coupled radial integral equations for each set of values of the good quantum numbers J , the total angular momentum, and Π , the parity of the channel. We add the partial-wave quantum numbers L', L to the sets i, j in the channel notation (19) to abbreviate the T -matrix (and V -matrix) elements as follows:

$$T_{nL}^{n'L'(J)} \equiv T_{ij} . \quad (42)$$

For channel j , L takes the values

$$|J-l| \leq L \leq J+l . \quad (43)$$

A further restriction on L is imposed by parity. The only channels that couple to the entrance channel are those with natural parity

$$\Pi(L+l) = \Pi(J) . \quad (44)$$

The coupled equations are

$$T_{ij}(q, k_j) = V_{ij}(q, k_j) + \sum_l \int_0^\infty dq' q'^2 V_{il}(q, q') G_l(q'^2) \times T_{ij}(q', k_j) , \quad (45)$$

$$T_{ij}(x_{in}, k_j) = V_{ij}(x_{in}, k_j) + \sum_l \sum_{n'=2}^{N+1} w_{n'-1} [x_{ln'}^2 V_{il}(x_{in}, x_{ln'}) T_{ij}(x_{ln'}, k_j) - k_l^2 V_{il}(x_{in}, k_l) T_{ij}(k_l, k_j)] \times \left[\frac{1}{2} (k_l^2 - x_{ln'}^2) \right]^{-1} - i\pi k_l V_{il}(x_{in}, k_l) T_{ij}(k_l, k_j) . \quad (48)$$

Here we have turned the principal-value integral into a regular integral²¹ by subtracting the on-shell value of the integrand using the identity

$$\mathcal{P} \int_0^\infty dq / (k_l^2 - q^2) = 0 , \quad (49)$$

thus removing the singularity at $q = k_l$. The final form of the equations to be solved is

$$T_{ij}(x_{in}, k_j) = V_{ij}(x_{in}, k_j) + \sum_l \sum_{n'=1}^{N+1} K_{il}(x_{in}, x_{ln'}) \times T_{ij}(x_{ln'}, k_j) . \quad (50)$$

The kernels are

$$K_{il}(x_{in}, x_{ln'}) = W_{ln} V_{il}(x_{in}, x_{ln'}) , \quad (51)$$

where, denoting the principal value by \mathcal{P} ,

$$G_l(q^2) = \mathcal{P} \frac{1}{\frac{1}{2}(k_l^2 - q^2)} - \frac{i\pi}{k_l} \delta(k_l - q) , \quad (46)$$

$$k_l^2 = 2(E + \epsilon_l) .$$

The momenta labeled by q are off shell and can take arbitrary values. The on-shell momenta k_l are the momenta of the external electron for the channels l .

To solve the equations numerically the q' integration is replaced by an N -fold quadrature sum²⁰ with weights w_r and coordinates q_r , $r = 1, \dots, N$. The coupled equations become a set of algebraic equations which can be written in terms of new coordinates x_{ln} in which the on- and off-shell notations are combined:

$$x_{ln} = k_l, \quad n = 1 \\ = q_{n-1}, \quad n = 2, \dots, N+1 . \quad (47)$$

The equations involve potential matrix elements $V_{il}(x_{in}, x_{ln'})$ that are typically off shell. The solution vector $T_{ij}(x_{in}, k_j)$ contains half-on-shell elements in addition to the physical on-shell elements that we are interested in:

where the superweights W_{ln} are obtained from (48):

$$W_{ln} = x_{ln}^2 w_{n-1} \left[\frac{1}{2} (k_l^2 - x_{ln}^2) \right]^{-1}, \quad n = 2, \dots, N+1 \\ = -k_l^2 \sum_{n'=2}^{N+1} w_{n'-1} \left[\frac{1}{2} (k_l^2 - x_{ln'}^2) \right]^{-1} - i\pi k_l, \quad n = 1 . \quad (52)$$

For solving the equations we use the matrix operations symbolized by the notation

$$T = (1 - K)^{-1} V . \quad (53)$$

If the calculation is carried out at any energy for which not all the channels are open, then the Green's functions for the closed channels are not singular and the subtraction procedure based on (49) is confined to the open channels.

V. TWO-ELECTRON POTENTIAL MATRIX ELEMENTS

The potential matrix elements (16) involved in the calculation are of three kinds: matrix elements of the core potential v_1 , direct and exchange matrix elements of the first-order potential v_3 , and the complex-polarization-potential matrix elements. In this section we describe the details of the calculation for v_3 .

The partial matrix elements arise from inverting the definition (20) with T replaced by v_3' :

$$V_{nL}^{n'L'(J)}(k', k) = \int d\hat{k}' \int d\hat{k} \sum_{MmM'm'} \langle L', M' | \hat{k}' \rangle C_{L'l'j}^{M'm'K} \langle \vec{k}'; n', l', m' | v_3' | n, l, m; \vec{k} \rangle C_{LU}^{MmK} \langle \hat{k} | L, M \rangle . \quad (54)$$

For charged targets we use the representation in terms of Coulomb functions $|\chi^{(\pm)}(\vec{k})\rangle$, which become plane waves $|\vec{k}\rangle$ in the uncharged case. For the direct matrix elements

$$\langle \chi^{(-)}(\vec{k}'); n', l', m' | v_3 | n, l, m; \chi^{(+)}(\vec{k}) \rangle = \int d^3 r_1 \int d^3 r_2 \chi^{(-)*}(\vec{k}', \vec{r}_1) \phi_{n'l'm'}^*(\vec{r}_2) v_3(|\vec{r}_1 - \vec{r}_2|) \phi_{nlm}(\vec{r}_2) \chi^{(+)}(\vec{k}, \vec{r}_1). \quad (55)$$

$$V_{nLi}^{n'L'I'(J)} = \frac{2}{\pi k' k} i^{L-L'} (-1)^{l+l'+J} \times \sum_{\lambda} \begin{Bmatrix} l & l' & \lambda \\ 0 & 0 & 0 \end{Bmatrix} \begin{Bmatrix} L & L' & \lambda \\ 0 & 0 & 0 \end{Bmatrix} \begin{Bmatrix} l & L & J \\ L' & l' & \lambda \end{Bmatrix} (\hat{L}\hat{L}'\hat{T}\hat{T}') R_{nn'LL'I'}^{(\lambda)}(k', k). \quad (56)$$

The symbols in parentheses and braces are, respectively, Wigner 3- j and 6- j symbols.

The radial integral is

$$R_{nn'LL'I'}^{(\lambda)}(k', k) = \int dr_1 \int dr_2 u_L(k', r_1) u_{n'l'}(r_2) \frac{r_1^\lambda}{r_2^{\lambda+1}} u_{nl}(r_2) u_L(k, r_1). \quad (57)$$

Here $u_L(k, r)$ is the regular Coulomb function $F_L(\eta, kr)$, where η is the Coulomb parameter

$$\eta = Z/k. \quad (58)$$

u_{nl} is the radial bound-state function. The radial integral is expressed in terms of one-dimensional quadrature sums in Appendix A. Its computation is very fast. For a dipole transition the r_2 integral behaves like r_1^{-2} for large r_1 . Hence, the r_1 integration converges very slowly. It is necessary to integrate so far in the radial dimension that u_L has its asymptotic form

$$u_L(k, r) = \sin(kr - L\pi/2) - \eta \ln 2kr + \sigma_L, \quad (59)$$

where σ_L is the Coulomb phase shift.

To generate the exchange matrix elements we apply the space-exchange operator to (55). The partial-wave reduction gives

$$V_{nLi}^{n'L'I'(J)} = \frac{2}{\pi k' k} i^{L-L'} (-1)^{l+l'+J} \sum_{\lambda} \begin{Bmatrix} l & L' & \lambda \\ 0 & 0 & 0 \end{Bmatrix} \begin{Bmatrix} L & l' & \lambda \\ 0 & 0 & 0 \end{Bmatrix} \begin{Bmatrix} l & L & J \\ l' & L' & \lambda \end{Bmatrix} (\hat{L}\hat{L}'\hat{T}\hat{T}') R_{nn'L'I'L'}^{(\lambda)}(k', k). \quad (60)$$

Here the r_1 integration converges much more quickly for all transitions.

For uncharged targets it is possible to perform the integrations in Eq. (55) [see Eqs. (29) to (32)]. We can thus work entirely in terms of momentum-space closed-form expressions. The calculation for the direct case is faster than the numerical integration involved in constructing (56) if the Slater expansion (17) of the orbitals is not too complicated.

The partial-wave direct matrix elements for a Slater pair described by (31) are

$$V_{nLi}^{n'L'I'(J)} = \sum_{l'', l''', \lambda} (2\pi^2)^{-1} i^{l+l''} (\hat{L}\hat{L}'\hat{T}\hat{T}') (\hat{l}''')^2 (\hat{l}'')^3 \left[\frac{(2l'')!}{(2\lambda)! [(2(l''-\lambda))!]} \right]^{1/2} \left[\sum_N g_{l''\lambda}^{Nl''} (k', k) \right] A_{Ll'l''l'''}^{L'I'(J)\lambda}, \quad (61)$$

$$A_{Ll'l''l'''}^{L'I'(J)\lambda} = (-1)^{J+l''+l'''+\lambda} \begin{Bmatrix} L & l'' & L' \\ l' & J & l \end{Bmatrix} \begin{Bmatrix} L & l'' & L' \\ l''-\lambda & l''' & \lambda \end{Bmatrix} \begin{Bmatrix} l'' & l' & l \\ 0 & 0 & 0 \end{Bmatrix} \begin{Bmatrix} L' & l''' & l''-\lambda \\ 0 & 0 & 0 \end{Bmatrix} \begin{Bmatrix} L & l''' & \lambda \\ 0 & 0 & 0 \end{Bmatrix}, \quad (62)$$

and

$$g_{l''\lambda}^{Nl''} (k', k) = 2\pi \int_{-1}^1 du P_{l''}(u) (k')^{l''-\lambda} k^\lambda K^{-(l''+2)} g_{l''}^N(K). \quad (63)$$

The Slater pair reduced matrix element $g_{l''}^N(K)$ is given by Eq. (30). The integral (63) requires a large amount of computing time for large values of l''' (large J). It is a major determining factor of the time for the overall computation.

The exchange matrix elements for a Slater pair (31) are

$$V_{nLi}^{n'L'I'(J)} = \sum_{\lambda, \lambda', l'', l''', \delta} (2\pi^2)^{-1} i^{l+l'} \hat{L}\hat{L}'\hat{T}\hat{T}'^2 (\hat{l}'')^2 (\hat{l}''')^2 \delta^2 \times (4\pi)^{-1} \left| \frac{(2l)!(2l')!}{(2\lambda)!(2\lambda')! [2(l-\lambda)]! [2(l'-\lambda')]!} \right|^{1/2} (-1)^{l+l'+L+L'+J} \times \begin{Bmatrix} L & l'' & l''' & l'' & L' \\ l' & l'-\lambda' & \delta & l-\lambda & J \end{Bmatrix} \begin{Bmatrix} l'' & l''' & \delta \\ 0 & 0 & 0 \end{Bmatrix} \begin{Bmatrix} \lambda' & \lambda & \delta \\ 0 & 0 & 0 \end{Bmatrix} \begin{Bmatrix} l'-\lambda' & l''' & L \\ 0 & 0 & 0 \end{Bmatrix} \times \begin{Bmatrix} l'' & l-\lambda & L' \\ 0 & 0 & 0 \end{Bmatrix} (k')^{l'-\lambda'} k^{l-\lambda} Z_{nl''l'''}^{n'l'l''}(\lambda+\lambda')(k', k), \quad (64)$$

where the symbol in braces is the Wigner 12- j symbol of the first kind²² and

$$Z_{nll'}^{n'l'l'(\Lambda)}(k', k) = \int_0^\infty dx x^\Lambda g_{l'l'}^{n'}(k', x) g_{ll'}^n(k, x). \quad (65)$$

The reduced matrix element $g_{ll'}^n$ is defined from $g_{l'l'}^n$ (30) by

$$g_{ll'}^n(|\vec{k} + \vec{x}|) = \sum_{l', m'} g_{l'l'}^n(k, x) \langle \hat{x} | l', m' \rangle \langle l', m' | \hat{k} \rangle. \quad (66)$$

The expression (64) is given for completeness. Present calculations use (60).

VI. EXTENSION TO THE INDEPENDENT-PARTICLE MODEL

In order to treat real one-electron atoms more accurately we can relax the inert core approximation sufficiently to allow electron exchange with particles in the closed-shell core. We do not allow configurations in which core electrons are promoted to excited states (core excitations).

Assuming an N -electron target it is convenient to partition the total Hamiltonian of the problem as follows:

$$H(x) = H_T(\bar{x}_i) + \bar{H}(x_i) + \sum_{\substack{j=0 \\ j \neq i}}^N r_{ij}^{-1}. \quad (67)$$

Here x stands for the set x_0, \dots, x_N of coordinates. x_i represents the space and spin coordinates \vec{r}_i and σ_i , respectively, of one electron. The notation \bar{x}_i represents the set x with the coordinate x_i removed. The Hamiltonian of the N -electron target is H_T and

$$\bar{H}(x_i) = K_i - N r_i^{-1} \quad (68)$$

is the sum of the one-electron kinetic-energy operator for coordinate \vec{r}_i and the potential felt by electron i from the target nucleus. The Hamiltonian is taken to be spin independent, and the target atom is assumed uncharged.

The wave function $\Psi^{(+)}$ of the scattering problem is defined by

$$(E - H)\Psi^{(+)} = 0. \quad (69)$$

Target wave functions Φ which are antisymmetric satisfy

$$(\epsilon_\Phi - H_T)\Phi = 0. \quad (70)$$

After making an antisymmetric multichannel expansion of $\Psi^{(+)}$ as a linear combination of products of target states and distorted waves $u_\Phi^{(+)}$ we obtain the following set of coupled equations for the $u_\Phi^{(+)}$ from Eq. (69):

$$\sum_{\Phi'} \left\{ \left[[E_\Phi - \bar{H}(\vec{r}_0)] \delta_{\Phi\Phi'} + V_{\Phi\Phi'}^D(x_0) \right] \langle x_0 | u_{\Phi'}^{(+)} \rangle + \int dx_1 V_{\Phi\Phi'}^E(x_0, x_1) \langle x_1 | u_{\Phi'}^{(+)} \rangle \right\} = 0. \quad (71)$$

The direct potential matrix element is

$$V_{\Phi\Phi'}^D(x_0) = N \int d\bar{x}_0 \langle \Phi | \bar{x}_0 \rangle r_{01}^{-1} \langle \bar{x}_0 | \Phi' \rangle, \quad (72)$$

and the exchange potential matrix element is

$$V_{\Phi\Phi'}^E(x_0, x_1) = N \int d\bar{x}_{01} \langle \Phi | \bar{x}_0 \rangle [E - H(x)] \langle \bar{x}_1 | \Phi' \rangle. \quad (73)$$

E_Φ is the energy of the external electron in the reaction channel specified by the target state Φ . The integral is taken over all coordinates except x_0 and x_1 .

With the use of independent-particle determinants for the states $\Psi^{(+)}$ and Φ the momentum-space potential matrix elements are

$$\langle \vec{k} | V_{\Phi\Phi'}^D | \vec{k}' \rangle = (2\pi)^{-3} \sum_i \int d^3 r_0 \int d^3 r_1 e^{-i\vec{k} \cdot \vec{r}_0} a_i^*(\vec{r}_1) r_{01}^{-1} b_i(\vec{r}_1) e^{i\vec{k}' \cdot \vec{r}_0} \langle \mu | \mu' \rangle \langle \mu_a | \mu_b \rangle, \quad (74)$$

$$\langle \vec{k} | V_{\Phi\Phi'}^E | \vec{k}' \rangle = (2\pi)^{-3} \sum_i \int d^3 r_0 \int d^3 r_1 e^{-i\vec{k} \cdot \vec{r}_0} a_i^*(\vec{r}_1) (E - \epsilon_a - \epsilon_b - r_{01}^{-1}) b_i(\vec{r}_0) e^{i\vec{k}' \cdot \vec{r}_1} \langle \mu | \mu_b \rangle \langle \mu_a | \mu' \rangle. \quad (75)$$

Here a_i and b_i stand for the i th orbitals in the determinants Φ and Φ' , respectively, ϵ_a and ϵ_b are the corresponding single-particle energies, μ_a and μ_b are the corresponding spin projections, and μ and μ' are the spin projections for the external electrons with momenta \vec{k} and \vec{k}' , respectively.

The spin-projection overlaps may be eliminated from (74), since they simply prohibit spin flip. The direct matrix element is a sum of matrix elements for each target electron. In our model $b_i = a_i$ for all of the core electrons. We group the exchange terms (73) into two classes. The first one involves the active electron, for which the exchange potential is given in terms of the orbitals ϕ_i and ϕ_j (with the use of the notation of Sec. II) by

$$\langle \vec{k}, \phi_i | v_3^E | \phi_j, \vec{k}' \rangle = (-1)^S \langle \vec{k}, \phi_i | (\epsilon_i + \epsilon_j + v_3 - E) P_r | \phi_j, \vec{k}' \rangle. \quad (76)$$

This exchange potential is analogous to the one in the pure three-body problem of Eq. (2). There is now an additional exchange potential coming from the contributions of the core electrons to Eq. (75). We have an exchange potential for each closed shell s , so that the matrix element of the core-exchange potential is

$$\langle \vec{k} | v_1^E | \vec{k}' \rangle = - \sum_s (2l_s + 1) \langle \vec{k}, \phi_s | (2\epsilon_s + v_s - E) P_r | \phi_s, \vec{k}' \rangle, \quad (77)$$

where the shell orbital, orbital angular momentum, and energy are given, respectively, by ϕ_s , l_s , and ϵ_s , and v_s is the Coulomb potential between the external electron and a core electron.

We can now start the coupled-channels optical formalism from the analog of Eq. (2), which is

$$[E^{(+)} - (K_1 + K_2 + v'_1 + v_2 + v'_3)]\Psi_{nS}^{(+)} = 0, \quad (78)$$

where the multichannel expansion of $\Psi_{nS}^{(+)}$ is not antisymmetrized and

$$\begin{aligned} v'_1 &= v_1 + v_1^E, \\ v'_3 &= v_3 + v_3^E, \end{aligned} \quad (79)$$

with the operators v_3^E and v_1^E defined by (76) and (77). Equation (6) is replaced by

$$v = v'_1 + v_2 + v'_3. \quad (80)$$

The static core potential v_1 includes the Coulomb potential of the nucleus.

With the use of the notation (31) for a pair of Slater functions arising from the product of two orbitals, the static contribution to the core potential of a closed shell with principal and orbital quantum numbers n, l is

$$v_{nl}(K) = 2(2l+1) \frac{1}{2\pi^2 K^3} \sum_M C_M(M-1)! \text{Im} \frac{1}{(\alpha_M + iK)^M}. \quad (81)$$

Here one of the nuclear charges has been used to subtract the singularity at $K=0$ in the matrix elements for the active electron. If there are $N-1$ electrons in the core we use $N-1$ charges to subtract the $K=0$ singularities in the terms (81). Any remaining charges give an overall Coulomb potential for a charged target

$$v_C(K) = (Z - N)/(2\pi^2 K^2), \quad (82)$$

where Z is the charge of the nucleus. If the target is charged the Coulomb representation (56) must be used for the direct matrix elements of the interaction of the incident electron with the active electron, since the closed-form expression (61) is the plane-wave representation of the coupling potential.

The partial-wave matrix element for a local central potential is described in Appendix B. Core-exchange matrix elements are calculated according to (60).

VII. POLARIZATION POTENTIALS

The complex-polarization potential is given exactly as the second term of (16). This expression involves the complete solution $\Psi_m^{(-)}$ of the problem for all three-body states m . To get the polarization potential in a form useful for calculation we must, therefore, approximate the $\Psi_m^{(-)}$ in some way, otherwise we merely have a rearrangement of the problem, not a solution. In fact the Coulomb three-body problem is so difficult that its solution is best approached by an iterative interaction of theory and experiment. It is at this point that the iterative process enters the present theory.

Investigations have shown that the polarization potential for discrete Q -space channels converges quite rapidly as the energy of the Q -space state becomes more and more

different from the energies of the states in P space. For example, in the one-channel (elastic) problem for hydrogen at 100 eV the $6p$ state contributes less than 1% to the polarization potential.²³ In these investigations the form chosen for $\Psi_m^{(-)}$ in the polarization potentials is just the Born approximation, that is, a wave function which is the product of the target state wave function and a plane wave for the incident electron. A study of other approximations and their comparison with this one have been carried out by Coulter and Garrett.²⁴

The above considerations suggest that most of the discrete Q -space contributions are insignificant at, say, a 1% accuracy level in actual computation. For discrete Q -space channels we are, therefore, interested in a finite set of channels called R space. The remainder of the Q space at our level of significance consists only of continuum channels and we denote this portion of the optical potential by $V^{(Q-R)}$. A further approximation we have made is the equivalent local approximation (see Appendix B). The equivalent local approximation to the second-order polarization potential for the excitation of an R -space channel has been discussed in Ref. 16. The fact that it gives an excellent comparison with experimental data^{18,19} is interesting from the point of view of the iterative interaction of experiment and theory. However, it is not essential to the theory, since it can be regarded as a mathematical approximation to the solution of the coupled-channels problem for the space $P+R$, and verified accordingly.^{25,26} The approximation of using the exact second-order potential for transitions from P space to R space and back is equivalent to solving the coupled-channels problem for $P+R$ with the approximation²⁵

$$R V^{(Q-R)} R = 0. \quad (83)$$

To model the continuum polarization potential $V^{(Q-R)}$ is more difficult. For the target continuum we do not have an exact calculation to which the optical potential provides an approximation. We are forced to use approximations to $\Psi^{(-)}(\vec{q}_1, \vec{q}_2)$, where \vec{q}_1 and \vec{q}_2 are the electron momenta in the ionized state, whose justification is their ability to reproduce experimental data. The real-polarization potential needs off-shell ionization matrix elements, which cannot be verified in comparison with ionization data. However, it is of second order in v_3 and we do not need great accuracy in comparison with the first-order P -space matrix elements.

The imaginary-polarization potential is an integral over Hermitian products of on-shell ionization amplitudes, which are directly related to ionization experiments. The integration over \vec{q}_1 and \vec{q}_2 means that it is necessary to have a good approximation only where the amplitudes are large. This is the case where the greater momentum $\vec{q}_>$ is much larger in magnitude than the lesser $\vec{q}_<$. The integration averages over details so it is not necessary to reproduce differential cross sections in detail. A good test of the continuum optical potential is its ability to reproduce the total ionization cross section, which is closely related¹ to $W(0)$. The Born-Oppenheimer approximation (with exchange), in which the slower electron always has a Coulomb wave orthogonalized to the relevant target states and the faster electron has a plane wave, is quite satisfactory²⁷ even as low as 50 eV. This approximation crudely describes screening, an important three-body effect. It is

the calculation of the continuum optical potential in this approximation that has already been successful for hydrogen with the P space consisting of the $1s$ state¹⁸ and the $1s$, $2s$, and $2p$ states.¹⁹ Its calculation is summarized below.

$$\langle \vec{k}_r | (U + iW) | \vec{k}_{r'} \rangle = -\frac{1}{2} \int_{-1}^1 du \int d^3q_1 \int d^3q_2 f^\dagger(\vec{k}_{r'} - \vec{k}_r + \vec{k}_i, \vec{q}_1, \vec{q}_2) [E^{(+)} - \frac{1}{2}(q_1^2 + q_2^2)]^{-1} f(\vec{k}_i, \vec{q}_1, \vec{q}_2), \quad (84)$$

where

$$u = \vec{k}_i \cdot (\vec{k}_{r'} - \vec{k}_r) / (k_i |\vec{k}_{r'} - \vec{k}_r|), \quad (85)$$

$$f(\vec{k}, \vec{q}_1, \vec{q}_2) = f_D(\vec{k}, \vec{q}_1, \vec{q}_2) + (-1)^S f_E(\vec{k}, \vec{q}_1, \vec{q}_2). \quad (86)$$

The direct and exchange amplitudes are, respectively,

$$f_D = \langle \vec{q}_>, \psi^{(-)}(\vec{q}_<) | v_3 | \phi_i, \vec{k} \rangle, \quad (87)$$

$$f_E = \langle \psi^{(-)}(\vec{q}_<), \vec{q}_> | v_3 | \phi_i, \vec{k} \rangle.$$

Because the continuum-state momenta \vec{q}_1 and \vec{q}_2 are just integration variables we need to consider only two types of numerator for the integrand of (84), denoted D_D and D_E in obvious notation. We divide the integration into two parts and make the Bonham-Ockhur peaking approximation where the plane waves occur with different coordinates. The first part has $q_1 \geq q_2$. For the second part we redefine \vec{q}_1 and \vec{q}_2 so that again $q_1 > q_2$. We now have

$$\begin{aligned} D_D &= (2\pi^2)^{-2} F(\vec{k}_r, \vec{k}_{r'}, \vec{q}_1, \vec{q}_2) \\ &\quad \times (|\vec{k}_r - \vec{q}_1|^{-2} |\vec{k}_{r'} - \vec{q}_1|^{-2} \\ &\quad + |\vec{k}_r - \vec{q}_2|^{-2} |\vec{k}_{r'} - \vec{q}_2|^{-2}), \\ D_E &= (2\pi^2)^{-2} F(\vec{k}_r, \vec{k}_{r'}, \vec{q}_1, \vec{q}_2) \\ &\quad \times (|\vec{k}_r - \vec{q}_1|^{-2} |\vec{k}_{r'} - \vec{q}_2|^{-2} \\ &\quad + |\vec{k}_r - \vec{q}_2|^{-2} |\vec{k}_{r'} - \vec{q}_1|^{-2}), \end{aligned} \quad (88)$$

where

$$F(\vec{k}_r, \vec{k}_{r'}, \vec{q}_1, \vec{q}_2) = \Delta_i^*(\vec{k}_r - \vec{q}_1, \vec{q}_2) \Delta_i(\vec{k}_{r'} - \vec{q}_1, \vec{q}_2), \quad (89)$$

$$\begin{aligned} \Delta_i(\vec{k}, \vec{p}) &= \int d^3q \langle \phi_i | \vec{q} \rangle \langle \vec{q} + \vec{k} | \\ &\quad \times \left[|\chi^{(+)}(\vec{p})\rangle - \sum_m |\phi_j\rangle \langle \phi_j | \chi^{(+)}(\vec{p})\rangle \right]. \end{aligned} \quad (90)$$

Here $\chi^{(+)}(\vec{p})$ is a Coulomb wave for an incident particle with momentum \vec{p} and the magnetic degeneracies of the bound state ϕ_j are denoted by m (other quantum numbers for j are the same as for i).

The orthogonalized Coulomb-plane-wave overlap Δ_i is expressed in terms of functions that are easily computed:

$$\Delta_i(\vec{k}, \vec{p}) = \left[D_i(\vec{k}, \vec{p}) - \sum_m D_j(0, \vec{p}) F_{ij}(\vec{k}) \right], \quad (91)$$

where

$$F_{ij}(\vec{k}) = \int d^3q \langle \phi_i | \vec{q} \rangle \langle \vec{q} + \vec{k} | \phi_j \rangle \quad (92)$$

The polarization potential is the second term on the right-hand side of (16). The Born-Oppenheimer approximation to the channel i diagonal matrix element is, in the equivalent local approximation (Appendix B),

$D_i(\vec{k}, \vec{p})$ is obtained for each term in the Slater expansion (17) of ϕ_i by the appropriate differentiations of the function²⁸ $D_0(\vec{k}, \vec{p})$,

$$\begin{aligned} D_0(\vec{k}, \vec{p}) &= (2\pi)^{-3} \int d^3r \exp(-i\vec{k} \cdot \vec{r}) \\ &\quad \times \exp(-\alpha r) \chi^{(+)}(\vec{p}, \vec{r}) \\ &= \frac{1}{\pi^2} \Gamma(1 - i\nu) e^{\pi\nu/2} \left[\frac{\nu(p + i\alpha)}{\alpha} \frac{B}{A} + 1 - i\nu \right] \\ &\quad \times \frac{\alpha}{B^2} \left[\frac{A}{B} \right]^{-i\nu}, \end{aligned} \quad (93)$$

where, for an attractive Coulomb potential for charge Z ,

$$\begin{aligned} \nu &= Z/k, \\ A &= k^2 - (p + i\alpha)^2, \\ B &= |\vec{k} - \vec{p}|^2 + \alpha^2. \end{aligned} \quad (94)$$

The method we have adopted for the integration (84) is the direct Diophantine²⁹ multidimensional integration. This method makes computation of the integrand very easy, since one can use Cartesian coordinates and partial-wave expansions are unnecessary. The principal-value integral for the real potential is again transformed to a regular integral by the subtraction (49).

VIII. NUMERICAL SOLUTION OF THE INTEGRAL EQUATIONS

The numerical methods involved in the solution of the coupled integro-differential equations for the close-coupling approximation in coordinate space are very well known.^{30,31} Since the present methods were developed with no previous experience of the difficulties peculiar to the atomic problem it is worth describing these difficulties and our solution of them. We also investigate the relative accuracy of the present method in comparison with the coordinate-space method.

The chief characteristic of the atomic problem is the electron-electron Coulomb potential, which introduces difficulties not present in nuclear physics where short-range forces are used. One of the major manifestations of the difficulty in coordinate space is the long range of the dipole coupling potentials, which means that the equations are coupled even in the external region. Since the boundary conditions are built into the integral equations this difficulty is overcome. However, the kernels for dipole and related transitions have more complicated structure than for monopole transitions.

The structure of the kernels is illustrated by Fig. 1, which shows profiles of the factors $k^2 V_{ij}^D(k, k')$ for the

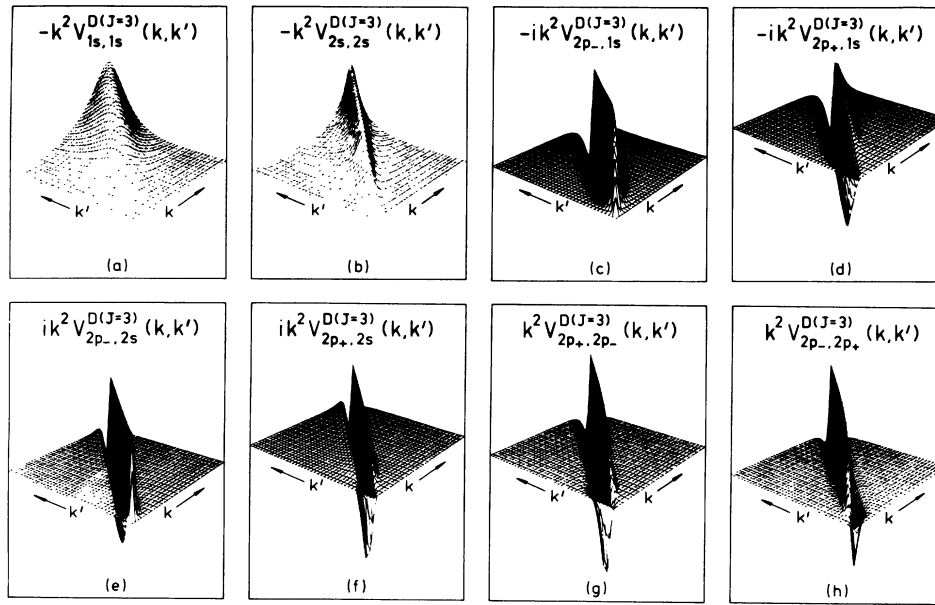


FIG. 1. Some of the direct parts of the off-shell potentials (multiplied by the Jacobian k^2) which make up the kernels of the $1s, 2s, 2p$ close-coupling equations in momentum space are shown for $J=3$. (\pm) subscripts on the p labels refer to the allowed values of L, L' , namely, $J \pm 1$. Both k and k' cover the range 0 to 20 a.u. Magnitudes of the different kernels are in arbitrary units.

direct potential matrix elements of v_3 for $J=3$ in the $1s, 2s, 2p$ P space for hydrogen. Exchange matrix elements have simpler structure, so that the numerical difficulties are due mainly to the direct terms.

There are two distinct types of potential profiles. The first is what one normally encounters in momentum space for standard short-range forms of potential. There is a characteristic peaking of the potential along the diagonal matrix elements $k=k'$. As one goes off the diagonal the potential profiles fall off at varying rates, depending on the particular potential. Thus, for example, the $1s-1s$ direct potential is more diffuse than the $2s-2s$ one. It is characteristic of the potentials coupling the channels that as orbitals from higher levels are coupled the potential becomes pronouncedly more peaked along the diagonal. We have not shown the $1s-2s$, $2p_- - 2p_-$, or $2p_+ - 2p_+$ potentials as their shape is typified by those of Figs. 1(a) and 1(b). For this type of potential profile coupled T -matrix equations in momentum space can be solved easily and accurately by discretizing the equations and subtracting out the Green's function singularity as discussed in Sec. IV.

However, in our initial calculations when we coupled in the $2p$ state, convergence of the solutions proved to be much poorer than was the case with $1s-2s$ coupling alone. The reason for this can be traced to the vastly different behavior of the off-shell potentials for dipole transitions, i.e., $1s-2p$ and $2s-2p$, and the transitions $2p_+ - 2p_-$ and $2p_- - 2p_+$. The behavior of these potentials is shown in Figs. 1(c)–1(h). Again all the structure is along a narrow band near the diagonal matrix elements. The difference here is that instead of a single peak there is a double peak structure. If we fix k and vary k' (or vice versa) then the kernels are very sensitive to variations in k' about $k=k'$. Again we note the trend that compared to the $1s$ dipoles of Figs. 1(c) and 1(d) the $2s$ dipoles have the same shapes

but are even more peaked about the diagonal. The $2p_+ - 2p_-$ and $2p_- - 2p_+$ transitions have shapes similar to the dipole profiles. Note, however, that while the partial-wave dipole potentials are imaginary, the $2p-2p$ ones are real. The reason why standard integration meshes are unsatisfactory when the $2p$ channel is coupled in is now obvious. Unless particular care is taken in the choice of mesh points it is quite possible to miss the important structure in the $2p$ coupled channels altogether.

Before discussing how to do this we should mention two other points concerning Fig. 1. First it may have come to the reader's attention that we have plotted $k^2 V^D(k, k')$ rather than V^D . The reason is that for the dipole-type transitions $V^D(k, k) \rightarrow k^{-1}$ as $k \rightarrow 0$ and so there is a pole at $k=k'=0$. The Jacobian factor k^2 ensures that the kernel is nonsingular at $k=0$. The other point to emerge from the profiles is their behavior for large k . It may appear from Figs. 1(a) and 1(b) that $k^2 V^D(k, k)$ is increasing with k . In fact, it is easy to show that the worst possible behavior for all the kernels is $k^2 V^D(k, k) \rightarrow \text{const}$ as $k \rightarrow \infty$.

At this stage we note that the complete kernel of (45) contains the factor $2/(k_l^2 - q'^2)$ in addition to $q'^2 V_{il}(q, q')$. This Green's function factor is responsible for convergence at large q' . The principal-value subtraction introduces an additional structure feature that increases the need to choose quadrature points that adequately represent the structure near the diagonal, namely, a sign change across the diagonal.

The integration mesh must adequately cover regions of large and small k in order to account for the diffuse structure for monopole transitions. At the same time it must include closely spaced points near the on-shell values of k in order to represent the detail of dipole and related kernels. Suppose we have a set of Gaussian quadrature points

u_j and weights w_j defined on the interval $[0,1]$. A standard conformal transformation for points z defined in the interval $[0,1]$ to points k defined on the interval $[0, \infty]$ is

$$k = \frac{az}{1-z}. \quad (95)$$

Here, half the k points have values less than a . For $z=0.5$, $k=a$. To cluster the points near b_1 and b_2 given by

$$\begin{aligned} z &= b_1 = 0.5 + b, \\ z &= b_2 = 0.5 - b, \end{aligned} \quad (96)$$

we transform $u \in [0,1]$ to z by

$$z = \frac{(u-b_1)^3 + (u-b_2)^3 + b_1^3 + b_2^3}{(1-b_1)^3 + (1-b_2)^3 + b_1^3 + b_2^3}. \quad (97)$$

The parameter a is chosen to be close to the on-shell value of k for dipole excitations. Values of b less than 1 cluster the points near a . Because of the rapid variation of some of the matrix elements in Fig. 1, the optimum value of b for the calculation is found to be in the vicinity of 0.1. The transformation (97) is only one of many possible. This form is chosen for its relative simplicity and ease of programming. In the integration the weights w_j are multiplied by the Jacobian dk/du_j ,

$$\frac{dk}{du} = \frac{a}{(1-z)^2} \frac{3(u-b_1)^2 + 3(u-b_2)^2}{(1-b_1)^3 + (1-b_2)^3 + b_1^3 + b_2^3}. \quad (98)$$

In the present calculation of coupling in the $1s, 2s, 2p$ -channel space of hydrogen, potential matrix elements are calculated to an absolute accuracy of 10^{-8} and a relative accuracy of at least 10^{-5} . The quality of the integration mesh and the solution of the integral equations for a particular value of J is judged by comparing calculations of the second-order on-shell T -matrix elements

$$\begin{aligned} T_{ij}^{(2)}(k_i, k_j) \\ = V_{ij}(k_i, k_j) + \int_0^\infty dq q^2 \sum_l V_{il}(k_i, q) G_l(q^2) V_{lj}(q, k_j) \end{aligned} \quad (99)$$

(a) with the use of the quadrature mesh, (b) performing the integral (99) by adaptive Romberg integration to a specified relative accuracy of 10^{-4} . All the integrals over non-dipole transitions are very convergent and one or two orders of magnitude more accurate than those involving dipole transitions. For the most difficult case, $J=0$, 2% or 3% accuracy is obtained at 54 and 100 eV with a 16-point mesh. 1% accuracy requires 24 points.

At energies in the range 50–200 eV, exchange matrix elements are negligible for $J \geq 13$. They are not calculated for these J values. The unitarized Born approximation, in which the real part of the Green's function $G_l(q^2)$ is neglected, is sufficiently accurate for $J \geq 23$. For the $1s-2p$ excitation the Born approximation to the T -matrix element is accurate to about 1% for J greater than about 25. Here the monopole potential matrix elements are less than 10^{-8} , but the coupling to the dipole channel results in monopole T -matrix elements that are not negligible. The Born approximation for monopole excitations is, therefore, invalid at the 1% level until J reaches quite large

values. We have used $J=80$ as the last value for which the UBA calculation is performed.

The accuracy of the present numerical methods is checked by a detailed comparison of the $1s, 2s, 2p$ close-coupling calculation with the coordinate-space calculations of Burke, Schey, and Smith³² and Kingston, Fon, and Burke¹¹ at 54.4 eV. Table I compares the contributions of the lower partial waves to the total cross section for each channel. Table II compares differential and total cross sections and angular correlation parameters for both 16- and 24-point meshes. Except for very small numbers in Table I for $J=1$, where there are clearly sensitive cancellations, the general estimate of 1% accuracy for 24 points and a few percent accuracy for 16 points is verified. The same is true for Table II except at large angles, where again there are severe cancellations of partial-wave contributions. A difference between the present calculation and the coordinate-space ones is that in the latter¹¹ exchange amplitudes are not calculated for $J > 8$, where the present calculation retains them up to $J=13$. We expect the resultant effect on the calculations of this difference in procedure to be small. Where the cross section is small at backward angles it may lead to a difference of a few percent.

Table I is useful for assessing the number of quadrature points necessary in the solution of the integral equations. For monopole transitions the partial-wave contributions are small for $J > 10$ in relation to the sum. Therefore, the greater error in the 16-point calculation is tolerable and 16 points are adequate. In any case, the 16-point contributions are identical to the 24-point contributions to the level of accuracy considered here. For the dipole transition the contributions for $J > 10$ are not negligible, but they are close to the Born approximation (given in parentheses in the column headed BSS). The small differences in accuracy are, therefore, again minimal and the use of 16-point quadratures is adequate. For $J \leq 10$ it is necessary to use 24 points for $\sim 1\%$ accuracy.

The computation reported here was done on the Prime 750 computer with double precision (64-bit words). (1 bit is a binary digit.) For comparable precision, execution times are roughly equal to those of the Control Data Corporation Cyber 173 computer or the Digital Equipment Corporation VAX 11/780 computer. The time is essentially proportional to the number of potential matrix elements to be calculated. For the pure three-state close-coupling calculation without polarization potentials, with the use of the coordinate-space methods of Eqs. (56), (57), and (60) and 24-point quadratures, the calculation takes 300 sec for each value of the total angular momentum J for the direct matrix elements and the same time, in addition, for the exchange matrix elements. Here the accuracy is about four figures. In order to obtain an accuracy of eight decimal places for the direct matrix elements we have used the momentum-space method (62) which for the 24-point calculation increases in time from 600 sec for $J=1$ to 2000 sec for $J=20$. The dimension of the potential matrix V_{ij} of (50) is in this case 100. Since the matrix is symmetric there are 5050 matrix elements to be calculated for each J value. The time is, therefore, roughly $\frac{1}{3}$ sec per matrix element for each J value. Note that for $J > 10$ we can halve the computation time by reducing the number of quadrature points from 24 to 16. The UBA re-

TABLE I. Contributions of the partial waves J to the total cross sections in the singlet (S) and triplet (T) states for 54.42-eV electrons in the $1s, 2s, 2p$ close-coupling approximation for hydrogen. Numbers in parentheses are obtained in the Born approximation. Column headings are as follows: 16, present 16-point calculation; 24, present 24-point calculation; BSS, Burke, Schey, and Smith (Ref. 32). Units are $10^{-4}\pi a_0^2$.

J	$1s(S)$			$1s(T)$			$2s(S)$		
	16	24	BSS	16	24	BSS	16	24	BSS
0	589	598	579	3993	3983	3979	51	50	49
1	93	93	89	2420	2432	2412	157	153	153
2	16	15	14	652	646	631	73	67	68
3	9	9	8	152	152	140	24	21	21
4	7	7	7	43	43	40	12	10	10
5	5	6	5	19	19	18	10	10	10
6	4	4	4	11	12	11	10	10	10
7	3	3	2	8	8	7	9	9	9
8	2	2		5	5		8	7	
9	1	1		4	4		6	6	
10	1	1		3	3		4	4	
11	1	1		2	2		3	3	
12	0	0		1	1		2	2	
13	0	0		1	1		2	2	
14	0	0		1	1		1	1	
15	0	0		1	1		1	1	

quires only ten matrix elements for each J value and the time is correspondingly shorter. The time to solve 100 complex linear equations for each J value is about 100 sec. The total time for the close-coupling calculation illustrated in Figs. 2–4 was roughly 7 h. The addition of nine polarization potentials representing Q space approximately doubles the computation time. The extra time is proportional to the number of polarization potentials.

IX. THE EFFECT OF Q SPACE

The coupled-channels optical method includes the effect of all channels outside P space by explicitly calculated polarization potentials, which are added to the first-order po-

tentials of the close-coupling approximation. The differential cross sections for the $1s, 2s, 2p$ channels of hydrogen at 54.42 eV are compared for the two methods in Figs. 2–4.

The inclusion of Q space has a large effect on inelastic differential cross sections (Fig. 2) where it raises the forward cross section and lowers it at backward angles. All the entrance-channel phenomena are related. This includes the total reaction cross section, which is, of course, underestimated in the three-state close-coupling method since reactions to only two channels are taken into account.

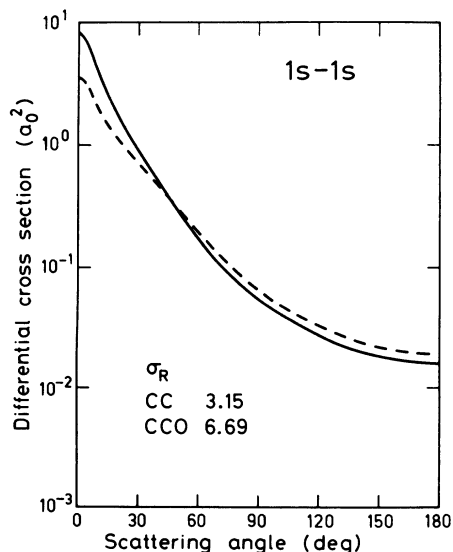


FIG. 2. $1s, 2s, 2p$ coupled-channels optical method (solid line) compared with three-state close coupling (dashed line) for the $1s-1s$ differential cross section at 54.42 eV.

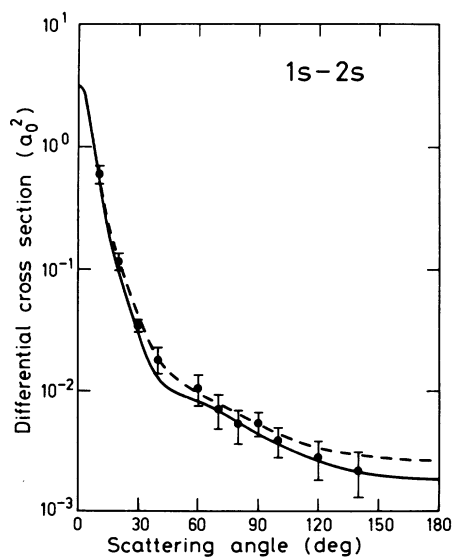


FIG. 3. $1s, 2s, 2p$ coupled-channels optical method (solid line) compared with three-state close coupling (dashed line) for the $1s-2s$ differential cross section at 54.42 eV. Experimental data are due to Williams (Ref. 34). Of his two estimates at each angle we have shown the one with the smaller statistical error.

TABLE I. (Continued.)

2s (T)			2p (S)			2p (T)		
16	24	BSS	16	24	BSS	16	24	BSS
32	31	30	34	36	35	54	53	52
160	157	154	5	6	24	28	31	38
186	173	175	164	168	169	130	138	139
111	101	100	296	301	302	380	392	394
53	45	45	341	345	347	609	621	624
30	25	25	324	328	329	715	725	728
24	21	21	282	284	286	708	716	719
21	20	20	234	236	237	637	643	647
19	17		191	191	(185)	545	545	(556)
15	15		154	156	(154)	452	457	(463)
12	12		124	126	(127)	370	374	(381)
9	9		101	102	(104)	299	303	(311)
7	7		81	82	(84)	242	245	(252)
5	5		65	66	(66)	196	198	(199)
4	4		53	53	(54)	159	160	(162)
3	3		43	43	(44)	128	130	(131)

In the spirit of the close-coupling approximation, square-integrable pseudostates may be added to the real states of P space to simulate the absorption of flux into Q space. The most comprehensive calculation of this type to date is that of Bransden *et al.*¹⁴ where the pseudostate basis contained four $l=0$ states and three with $l=1$. They were included in second-order polarization potentials calculated without taking account of exchange. Table III shows the total reaction cross section at 54.42 eV obtained by the various methods. This is a test of the adequacy of the description of Q space (which is not described at all in the close-coupling approximation, of course). The experi-

mental estimate of de Heer *et al.*³⁵ has been extrapolated from 50 to 54.42 eV by decreasing it in the same ratio as the total reaction cross sections for the present method at 50 and 54.42 eV.

The effect of Q space on the inelastic channels is a third-order effect in terms of the expansion of the T matrix in the electron-electron potential. It is quite small (Figs. 3 and 4), being of the order of 30% at backward angles and relatively much smaller at forward angles.

X. CONCLUSIONS

The momentum-space coupled-channels optical method takes into account all relevant effects in electron-atom scattering explicitly. Use of the momentum representation facilitates calculation of the polarization potentials representing Q -space effects. The numerical methods explained here enable the coupled-channels calculation to be done with sufficient accuracy.

The inclusion of Q -space effects in the coupled-channels calculation has a large effect on the results for the entrance channel, providing the increased forward scattering characteristic of polarization and enabling the total reaction cross section to be correctly calculated. It is important also in the details of inelastic phenomena.

Since the momentum-space calculation involves the inversion of a matrix, whose elements are essentially on- and off-shell Born amplitudes, it lends itself to very good approximations for discrete channels outside the basic P space within which scattering results are required in detail. This set of channels is projected by the operator R . It may be included, for example, by performing a coupled-channels calculation for the space $P+R$ with the omission of matrix elements of the operator $RV^{(Q-R)}R$. This is the essential approximation involved in representing R space by second-order optical potentials, but it does not make the equivalent-local approximation. Further matrix elements may be omitted, for example those for

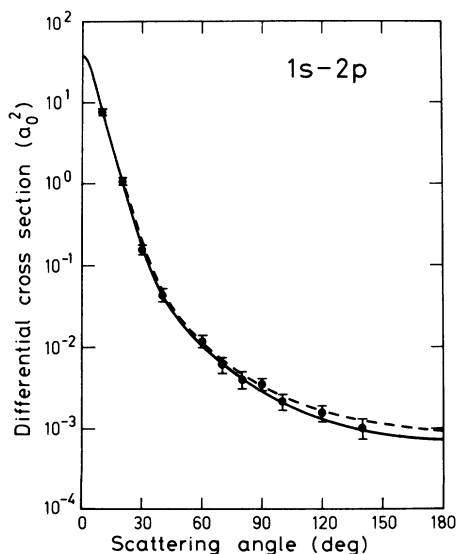


FIG. 4. $1s, 2s, 2p$ coupled-channels optical method (solid line) compared with three-state close coupling (dashed line) for the $1s-2p$ differential cross section at 54.42 eV. Experimental data are due to Williams (Ref. 34).

TABLE II. Differential and total cross sections for $2s$ and $2p$ excitations and angular correlation parameters λ and R for 54.42-eV electrons in the $1s, 2s, 2p$ close-coupling approximation for hydrogen. Column headings are as follows: 16, present 16-point calculation; 24, present 24-point calculation; KFB, Kingston, Fon, and Burke (Ref. 8); KLB, Kingston, Liew, and Burke (Ref. 33). Units are a_0^2 . Exponents of multiplication factors of 10 are indicated by superscripts.

θ	$2s$		$2p$		λ		R	
	16	24	16	24	16	24	16	24
0	3.43	3.22	3.85 ⁺¹	3.90 ⁺¹	1	1	0	0
10	6.38 ¹	5.76 ⁻¹	7.65	7.78	2.77 ⁻¹	2.82 ⁻¹	3.00 ⁻¹	3.00 ⁻¹
20	1.26 ⁻¹	1.22 ⁻¹	1.16	1.17	1.83 ⁻¹	1.92 ⁻¹	2.25 ⁻¹	2.25 ⁻¹
30	4.35 ⁻²	4.44 ⁻²	1.95 ⁻¹	1.97 ⁻¹	3.27 ⁻¹	3.40 ⁻¹	2.30 ⁻¹	2.30 ⁻¹
40	1.88 ⁻²	1.87 ⁻²	4.66 ⁻²	4.76 ⁻²	6.67 ⁻¹	6.79 ⁻¹	2.20 ⁻¹	2.21 ⁻¹
60	1.03 ⁻²	1.01 ⁻²	1.06 ⁻²	1.13 ⁻²	9.10 ⁻¹	9.20 ⁻¹	1.10 ⁻¹	1.10 ⁻¹
80	6.82 ⁻³	6.52 ⁻³	4.59 ⁻²	4.55 ⁻³	7.96 ⁻¹	8.00 ⁻¹	1.00 ⁻¹	1.12 ⁻¹
100	4.58 ⁻³	4.50 ⁻³	2.64 ⁻³	2.60 ⁻³	8.03 ⁻¹	8.01 ⁻¹	1.58 ⁻¹	1.63 ⁻¹
120	3.42 ⁻³	3.36 ⁻³	1.82 ⁻³	1.61 ⁻³	8.83 ⁻¹	8.71 ⁻¹	1.86 ⁻¹	1.67 ⁻¹
140	2.83 ⁻³	3.00 ⁻³	1.42 ⁻³	1.25 ⁻³	9.51 ⁻¹	9.59 ⁻¹	1.35 ⁻¹	1.16 ⁻¹
160	2.54 ⁻³	2.74 ⁻³	1.25 ⁻³	1.08 ⁻³	9.88 ⁻¹	9.84 ⁻¹	7.06 ⁻²	5.90 ⁻²
180	2.40 ⁻³	2.62 ⁻³	1.19 ⁻³	9.24 ⁻⁴	1	1	0	0
σ	3.38 ⁻¹	3.18 ⁻¹	2.80	2.84	1	1	0	0
								2.85

TABLE III. Total reaction cross sections (σ_R) for hydrogen at 54.42 eV. MS, present calculation; BSSR, Bransden *et al.* (Ref. 14); CC, three-state close coupling; Expt., extrapolation of de Heer *et al.* (Ref. 35).

Method	σ_R (a_0^2)
MS	6.69
BSSR	10.92
CC	3.15
Expt.	6.31 \pm 0.63

nondipole excitations, which are small.

Furthermore, the calculation time may be reduced by making relaxed approximations to T matrices for larger values of the total angular momentum quantum numbers J . We have shown, for example, that fewer quadrature points are needed for larger J . The method will enable a very large space of discrete channels to be included.

ACKNOWLEDGMENT

We would like to acknowledge support from the Australian Research Grants Scheme.

APPENDIX A: RADIAL INTEGRATION FOR EXCHANGE MATRIX ELEMENTS

The radial integral (57) has the form

$$R = \int dr_1 \int dr_2 f(r_1)g(r_2)r_<^\lambda / r_>^{\lambda+1}. \quad (\text{A1})$$

It is calculated as a sum over functions at quadrature points labeled by i with weights w_i ,

$$R = \sum_{i=1}^n w_i f_i (T_i / r_i^{\lambda+1} + S_i r_i^\lambda), \quad (\text{A2})$$

where T_i and S_i are given by the following recurrence relations:

$$T_i = T_{i-1} + w_i g_i r_i^\lambda, \quad T_0 = 0, \quad (\text{A3})$$

$$S_i = S_{i-1} - w_i g_i / r_i^{\lambda+1}, \quad S_0 = \sum_{i=1}^n w_i g_i / r_i^{\lambda+1}. \quad (\text{A4})$$

The sums T_i and S_0 are rapidly convergent because they contain at least one exponentially decaying radial bound-state function.

APPENDIX B: LOCAL, CENTRAL POTENTIALS IN THE ATOMIC CENTER-OF-MASS SYSTEM

The potential matrix elements coupling the various channels are, in general, a sum of local and nonlocal potentials $\langle \vec{k}' | V | \vec{k} \rangle$, whose form depends on the channel indices. The momentum-space equivalent of a local potential which is central in the atomic center-of-mass system is one that depends only on the magnitude K of the momentum transfer \vec{K} , given by

$$\vec{K} = \vec{k} - \vec{k}'. \quad (\text{B1})$$

The polarization potentials (16) are nonlocal, i.e., they cannot be written only as a function of K . Nevertheless, it has proven¹ useful to make a simplifying equivalent-local

approximation as follows. We define

$$U_{ij}(K) + iW_{ij}(K) = -\frac{1}{2}\delta_{ij} \int_{-1}^1 du \langle (\vec{K} + \vec{k}_j), \phi_i | V^{(Q)} | \phi_j, \vec{k}_j \rangle. \quad (\text{B2})$$

Here \vec{k}_j is the on-shell momentum for channel j . The spherical averaging is over angles defined by

$$u = \hat{K} \cdot \hat{k}_j. \quad (\text{B3})$$

We keep only the diagonal terms (B2). This is based on

$$U_{nLi}^{n'L'I'(J)}(k', k) = \delta_{nn'} \delta_{ll'} \int d\hat{k}' \int d\hat{k} \sum_{M, m, M', m'} \langle L', M' | \hat{k}' \rangle C_{L'I'J}^{M'm'K} U_{nl}(K) C_{LL'}^{MmK} \langle \hat{k} | L, M \rangle. \quad (\text{B4})$$

We make a multipole expansion of $U_{nl}(K)$,

$$U_{nl}(K) = \sum_{\lambda, \mu} \langle \hat{k}' | \lambda, \mu \rangle u_{n\lambda l}(k', k) \langle \lambda, \mu | \hat{k} \rangle \quad (\text{B5})$$

and substitute it into (B4) to obtain

$$U_{nLi}^{n'L'I'(J)}(k', k) = \delta_{nn'} \delta_{ll'} \delta_{ll'} u_{nLi}(k', k), \quad (\text{B6})$$

where $u_{nLi}(k', k)$ is obtained by inverting (B5):

the observation³⁶ that the off-diagonal terms are much smaller than the diagonal ones. They can certainly be neglected. If the orbital angular momentum l of the bound state in channel j is not zero, we average over the m components of l . Thus the polarization-potential matrix elements we use are labeled by n and l and are diagonal in the channel indices.

The partial-wave matrix element of the most general form of the local central potential occurring in this problem is, therefore, of the form (54),

$$u_{nLi}(k', k) = 2\pi \int_{-1}^1 dx U_{nl}(K) P_L(x), \quad (\text{B7})$$

$$x = \hat{k}' \cdot \hat{k}. \quad (\text{B8})$$

Note that the partial-wave matrix element of a local, central potential depends on the total angular momentum quantum number J only through the continuum-state orbital angular momentum L , which is related to J by (43) and (44).

- ¹I. E. McCarthy and A. T. Stelbovics, Phys. Rev. A **22**, 502 (1980).
²M. H. Mittleman and K. M. Watson, Phys. Rev. **113**, 198 (1959).
³R. A. Bonham, Phys. Rev. A **3**, 298 (1971); **3**, 1958 (1971).
⁴F. W. Byron, Jr. and C. J. Joachain, Phys. Rev. A **8**, 1267 (1973); **8**, 3266 (1973).
⁵I. H. Sloan and E. J. Moore, J. Phys. B **1**, 414 (1968).
⁶V. M. Burke and M. J. Seaton, Proc. Phys. Soc. (London) **77**, 199 (1961).
⁷W. B. Sommerville, Proc. Phys. Soc. (London) **82**, 446 (1963).
⁸B. C. Saha, A. S. Ghosh, and N. C. Sil, J. Phys. B **8**, 1627 (1975).
⁹B. C. Saha, J. Chaudhuri, and A. S. Ghosh, J. Phys. Soc. Jpn. **41**, 1716 (1976).
¹⁰N. C. Sil and B. C. Saha, J. Phys. Soc. Jpn. **42**, 721 (1977).
¹¹A. E. Kingston, W. C. Fon, and P. G. Burke, J. Phys. B **9**, 605 (1976).
¹²J. Callaway, M. R. C. McDowell, and L. A. Morgan, J. Phys. B **8**, 2180 (1975).
¹³T. Scott and B. H. Bransden, J. Phys. B **14**, 2277 (1981).
¹⁴B. H. Bransden, T. Scott, R. Shingal, and R. K. Roychoudhury, J. Phys. B **15**, 4605 (1982).
¹⁵R. A. Bonham, J. Chem. Phys. **36**, 3260 (1962); V. I. Ochkur, Zh. Eksp. Teor. Fiz. **45**, 734 (1963) [Sov. Phys.—JETP **18**, 503 (1964)].
¹⁶I. E. McCarthy, B. C. Saha, and A. T. Stelbovics, J. Phys. B **14**, 2871 (1981).
¹⁷I. E. McCarthy, B. C. Saha, and A. T. Stelbovics, Aust. J. Phys. **34**, 135 (1981).
¹⁸I. E. McCarthy, B. C. Saha, and A. T. Stelbovics, J. Phys. B **15**, L401 (1982).
¹⁹I. E. McCarthy and A. T. Stelbovics, J. Phys. B **16**, 1233 (1983).
²⁰C. T. Baker, *The Numerical Treatment of Integral Equations* (Clarendon, Oxford, 1977); P. M. Anselone, *Collectively Com-*

pact Operator Approximation Theory and Applications to Integral Equations (Prentice-Hall, Englewood Cliffs, N.J., 1971).

- ²¹This subtraction method of regularizing the equation was brought to our notice by I. R. Afnan. Although similar methods have been applied to improve convergence where kernel derivatives are unbounded (e.g., Ref. 20) as far as we are aware no discussion of the present method exists in the mathematical literature.
²²A. P. Jucys, I. B. Levinson, and V. V. Vanagas, *Mathematical Apparatus of the Theory of Angular Momentum* (Institute of Physics and Mathematics of the Academy of Sciences of the Lithuanian S. S. R., Mintis, Vilnius, 1960) [English translation: Israel Program for Scientific Translations Ltd., Jerusalem, 1962].
²³I. E. McCarthy, B. C. Saha, and A. T. Stelbovics, Phys. Rev. A **23**, 145 (1981).
²⁴P. W. Coulter and W. R. Garrett, Phys. Rev. A **23**, 2213 (1981).
²⁵I. E. McCarthy and A. T. Stelbovics, Aust. J. Phys. (in press).
²⁶I. E. McCarthy and A. T. Stelbovics, J. Phys. B **16**, 1611 (1983).
²⁷I. E. McCarthy and A. T. Stelbovics, Phys. Rev. A (in press).
²⁸E. Guth and C. J. Mullin, Phys. Rev. **83**, 667 (1951).
²⁹H. Conroy, J. Chem. Phys. **47**, 5307 (1967); A. T. Stelbovics and R. S. Watts (unpublished).
³⁰P. G. Burke and H. M. Schey, Phys. Rev. **126**, 147 (1962).
³¹P. G. Burke and K. Smith, Rev. Mod. Phys. **34**, 458 (1962).
³²P. G. Burke, H. M. Schey, and K. Smith, Phys. Rev. **129**, 1258 (1963).
³³A. E. Kingston, Y. C. Liew, and P. G. Burke, J. Phys. B **15**, 2755 (1982).
³⁴J. F. Williams, J. Phys. B **14**, 1197 (1981).
³⁵F. J. de Heer, M. R. C. McDowell, and R. W. Wagenaar, J. Phys. B **10**, 1945 (1977).
³⁶I. E. McCarthy and M. R. C. McDowell, J. Phys. B **12**, 3775 (1979).